ULTRASOUND NEWS

JULY 2021

Small testes: clinical characteristics and ultrasonographic findings

Dal Mo Yang[1], Hyeon-Il Choi[1], Hyun Cheol Kim[1], Sang Won Kim[1], Sung Kyung Moon[2], Joo Won Lim[2]

[1]Department of Radiology, Kyung Hee University Hospital at Gangdong, Seoul; [2]Department of Radiology, Kyung Hee University Hospital, Seoul, Korea

ULTRASONOGRAPHY

PICTORIAL ESSAY

https://doi.org/10.14366/usg.20133
pISSN: 2288-5919 • eISSN: 2288-5943
Ultrasonography 2021;40:455-463

The purpose of this pictorial essay is to describe the ultrasonographic and clinical findings of patients with small testes due to a wide range of causes. We retrospectively reviewed the ultrasonographic and clinical findings of various causes of small testes. We present various causes of small testes on ultrasonography including Klinefelter syndrome, testicular torsion, mumps orchitis, inguinal hernia, cryptorchidism, varicocele, and trauma. On ultrasonography, small testes in patients with testicular torsion, mumps orchitis, and trauma usually showed heterogeneous echogenicity. Atrophic testes were homogeneously hypoechoic in patients with cryptorchidism and inguinal hernia and were isoechoic to the normal testis in patients with varicocele. Klinefelter syndrome patients had small hyperechoic or hypoechoic nodules, but the echogenicity of the remnant portion of the testes was homogeneous. Ultrasonography is helpful for detecting small testes and for the differential diagnosis of the various possible causes of small testes.

Keywords: Testis; Small testes; Testicular atrophy; Ultrasonography; Color Doppler ultrasonography

Received: August 22, 2020
Revised: November 1, 2020
Accepted: November 3, 2020

Correspondence to:
Dal Mo Yang, MD, Department of Radiology, Kyung Hee University Hospital at Gangdong, 892 Dongnam-ro, Gangdong-gu, Seoul 05278, Korea

Tel. +82-2-440-6183
Fax. +82-2-440-6932
E-mail: dmy2988@daum.net

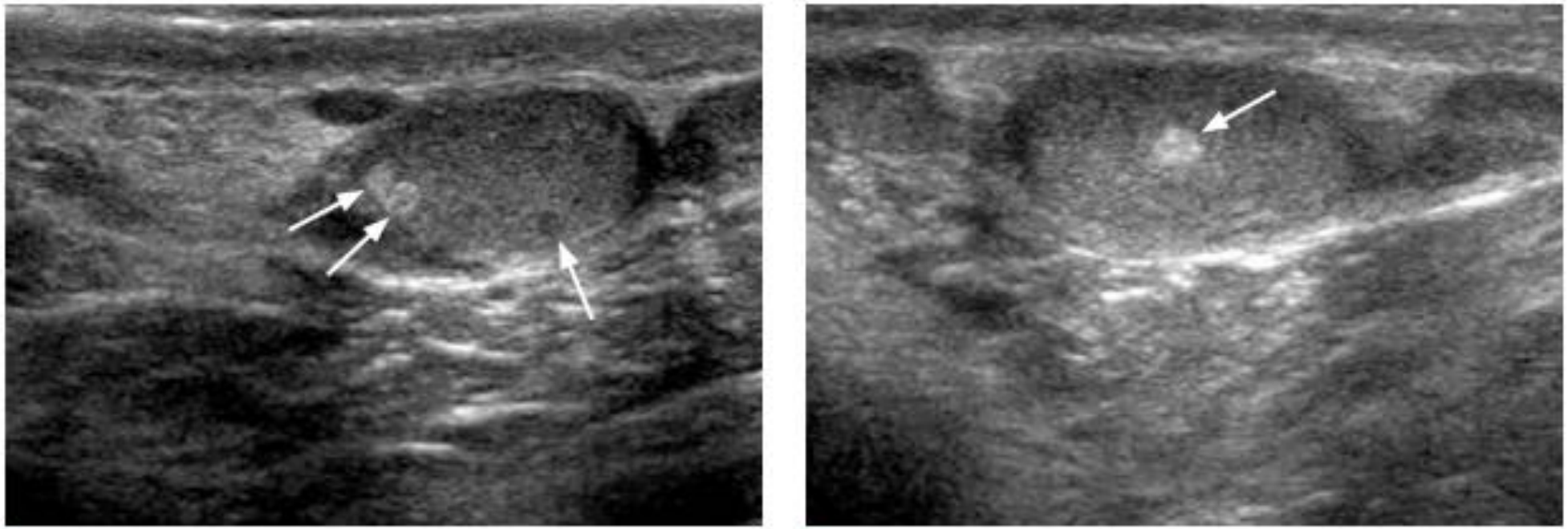

A B

Fig. 1. **A 28-year-old man with Klinefelter syndrome.**
A. Longitudinal ultrasonography shows a small right testis (0.5 mL) with two small hyperechoic lesions and a hypoechoic lesion in the testis (arrows). B. Longitudinal ultrasonography shows a small left testis (0.5 mL) with a small hyperechoic lesion (arrow).

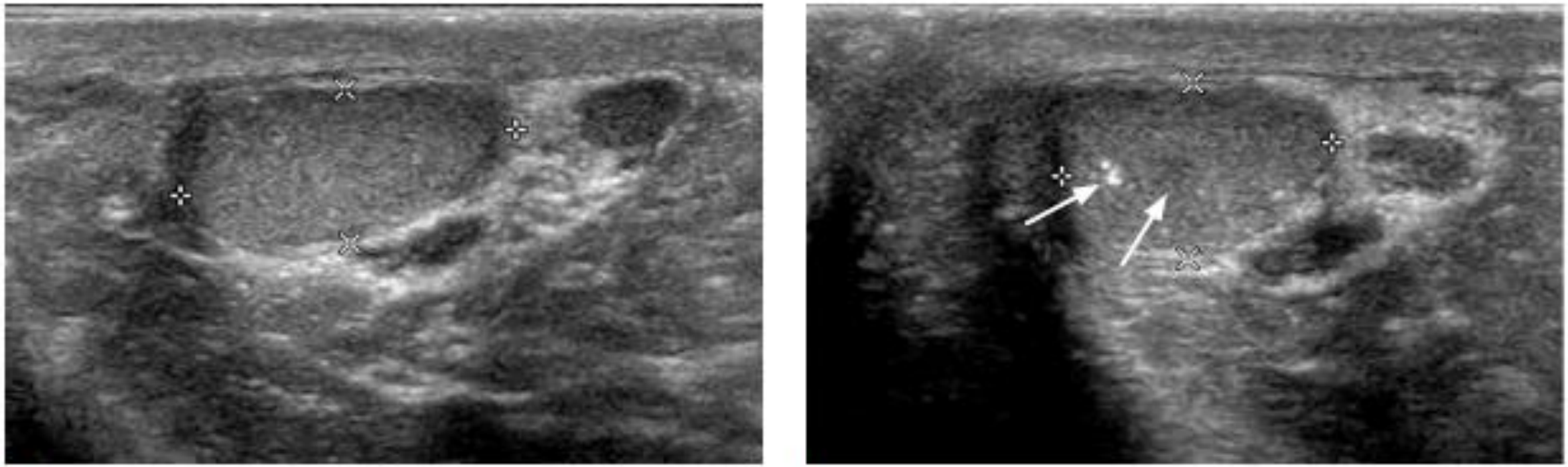

A B

Fig. 2. A 29-year-old man with Klinefelter syndrome.

A. Longitudinal ultrasonography shows a small right testis with normal echogenicity and a 0.4-mL testicular volume. B. Longitudinal ultrasonography shows a small left testis (0.5 mL) with internal hypoechoic and hyperechoic lesions (arrows).

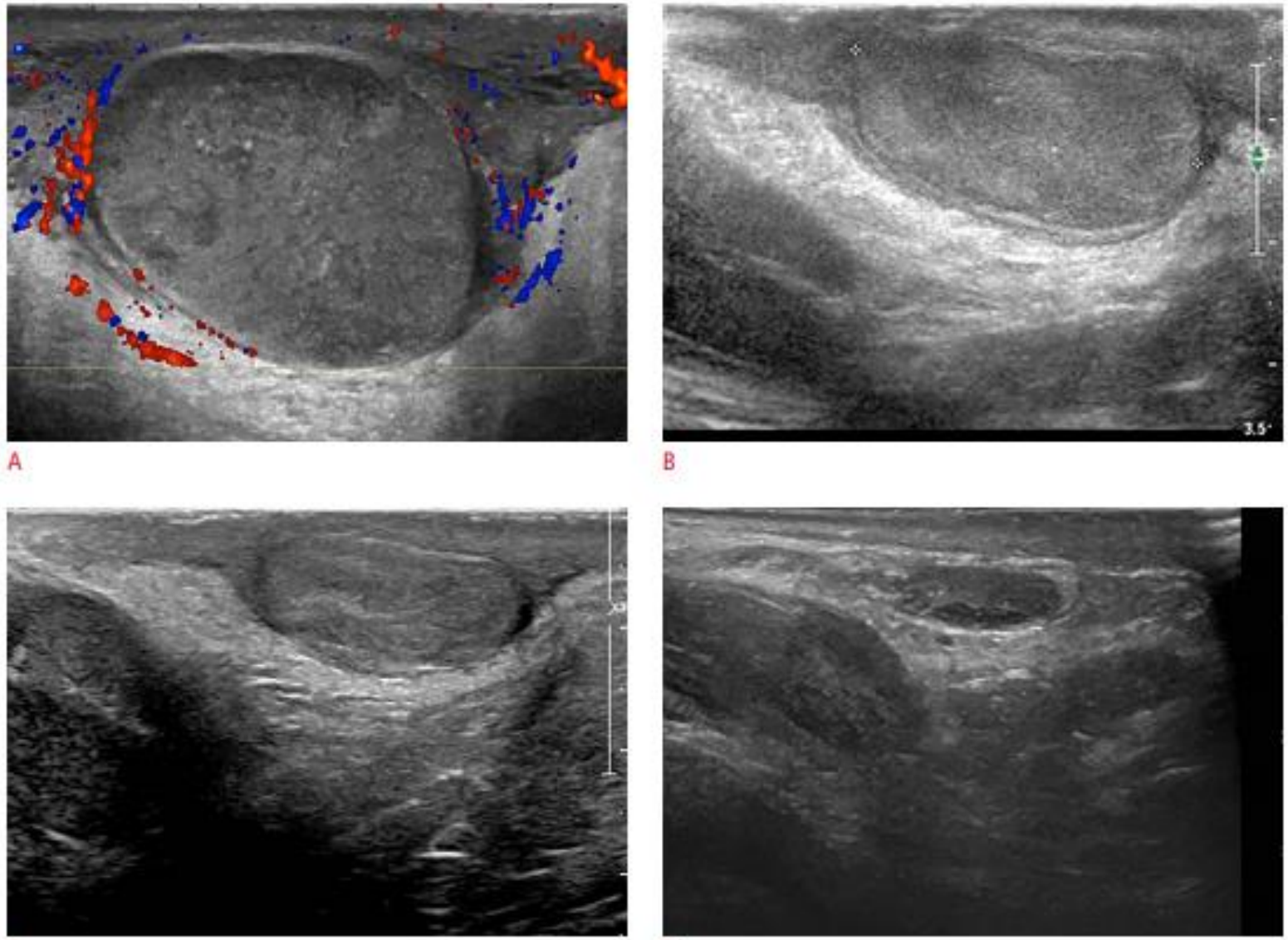

Fig. 3. A 14-year-old boy with left testicular torsion with orchiopexy.
A. Longitudinal color Doppler ultrasonography shows no blood flow in the enlarged left testis with heterogeneously low echogenicity and a 10.1-mL testicular volume. B–D. Follow-up longitudinal ultrasonography after orchiopexy demonstrates a gradual decrease in the volume of the left testis, showing heterogeneous echogenicity (B, 18 days later; C, 64 days; D, 134 days).

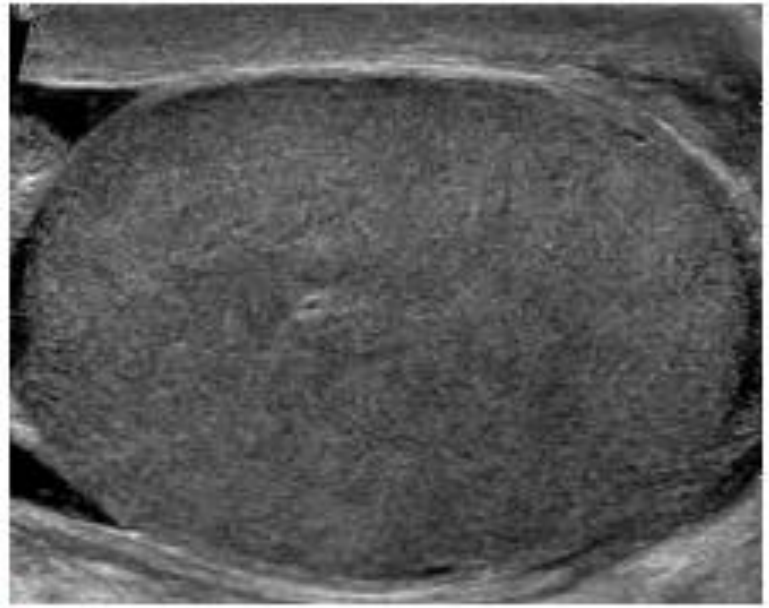

A

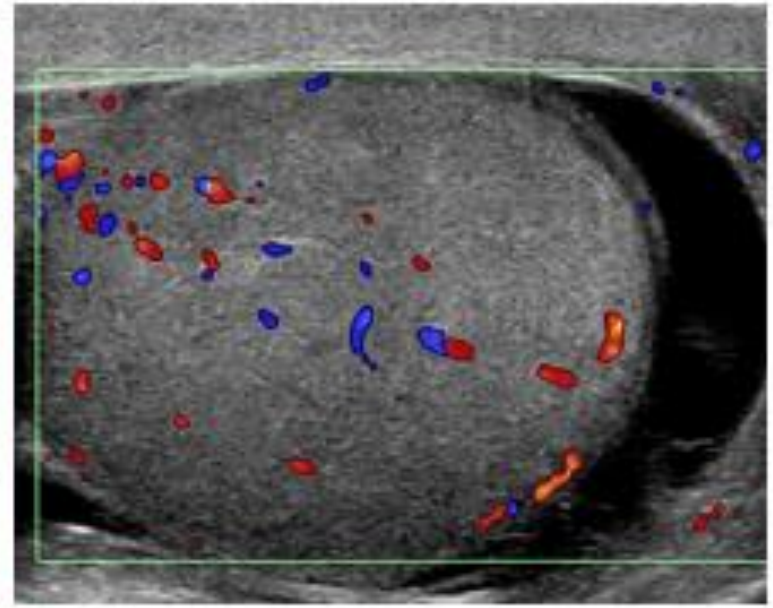

B

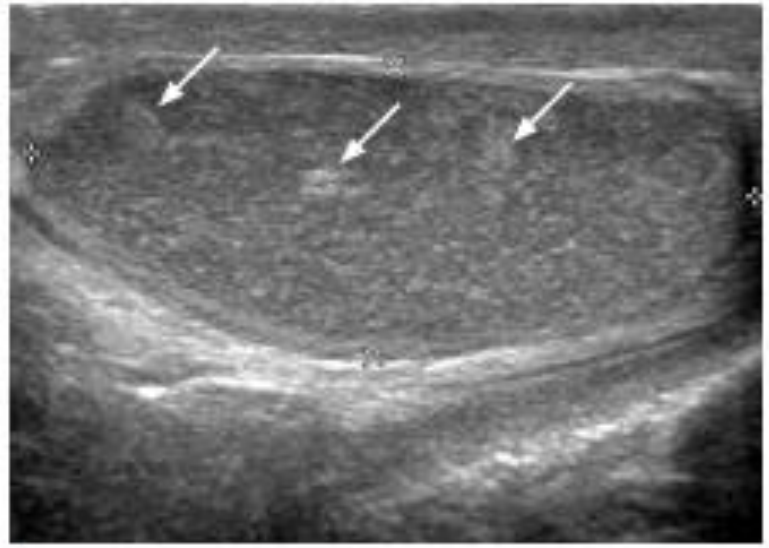

C

Fig. 4. **A 16-year-old boy with mumps orchitis.**
A. Longitudinal ultrasonography shows an enlarged hypoechoic right testis with a 35-mL testicular volume. B. Color Doppler ultrasonography shows increased blood flow in the enlarged testis. C. After 110 days, longitudinal ultrasonography shows a right testis with reduced volume of 5.2 mL. The testis is heterogeneously hypoechoic with multiple hyperechoic foci (arrows) on ultrasonography.

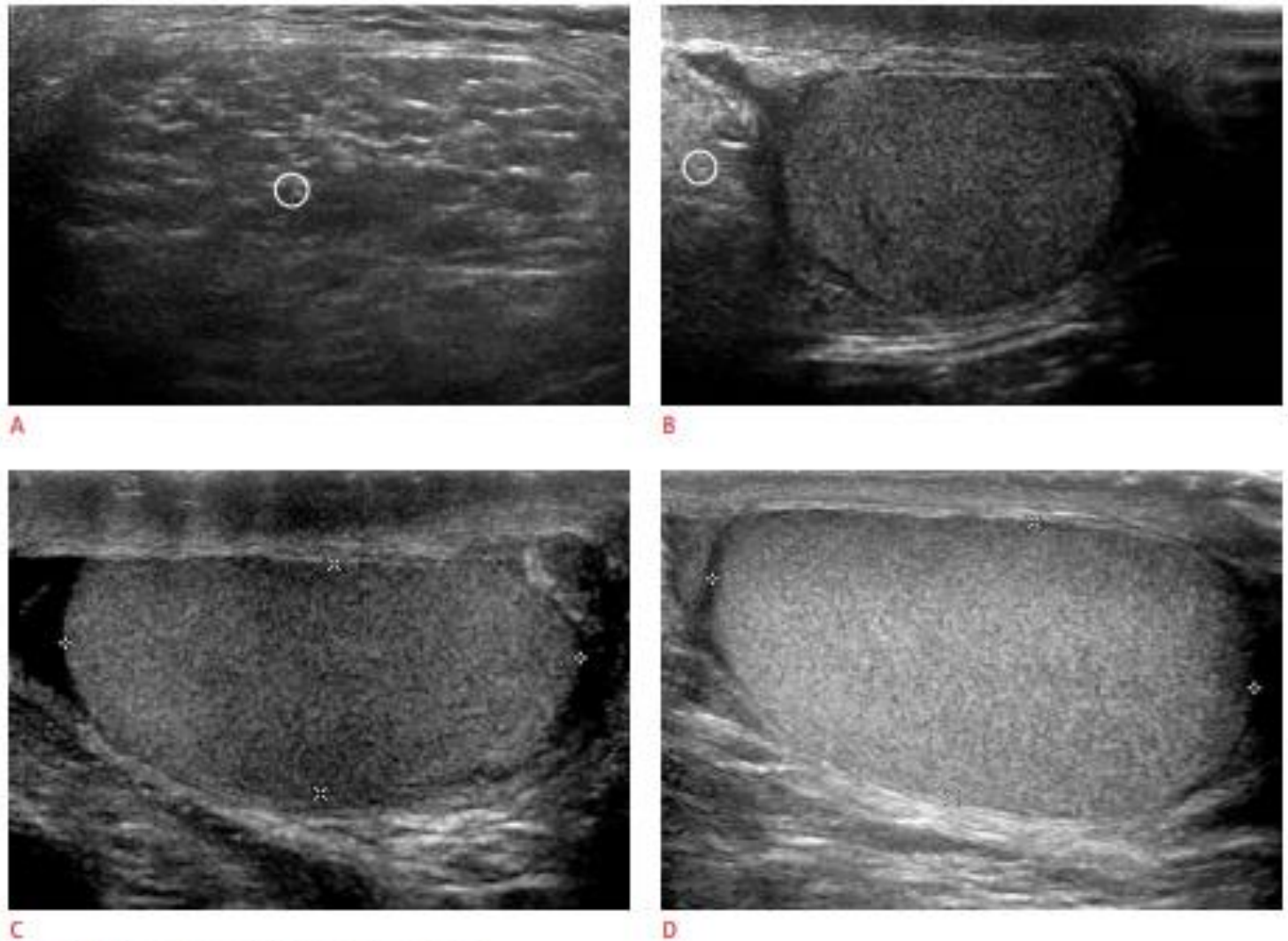

Fig. 5. A 31-year-old man with left inguinal hernia.
A. Longitudinal ultrasonography shows herniated omental fat presenting as a heterogeneously hyperechoic mass in the left inguinal canal. B, C. Longitudinal ultrasonography shows a small hypoechoic left testis. D. Longitudinal ultrasonography shows a normal right testis. Circles indicate omental fat.

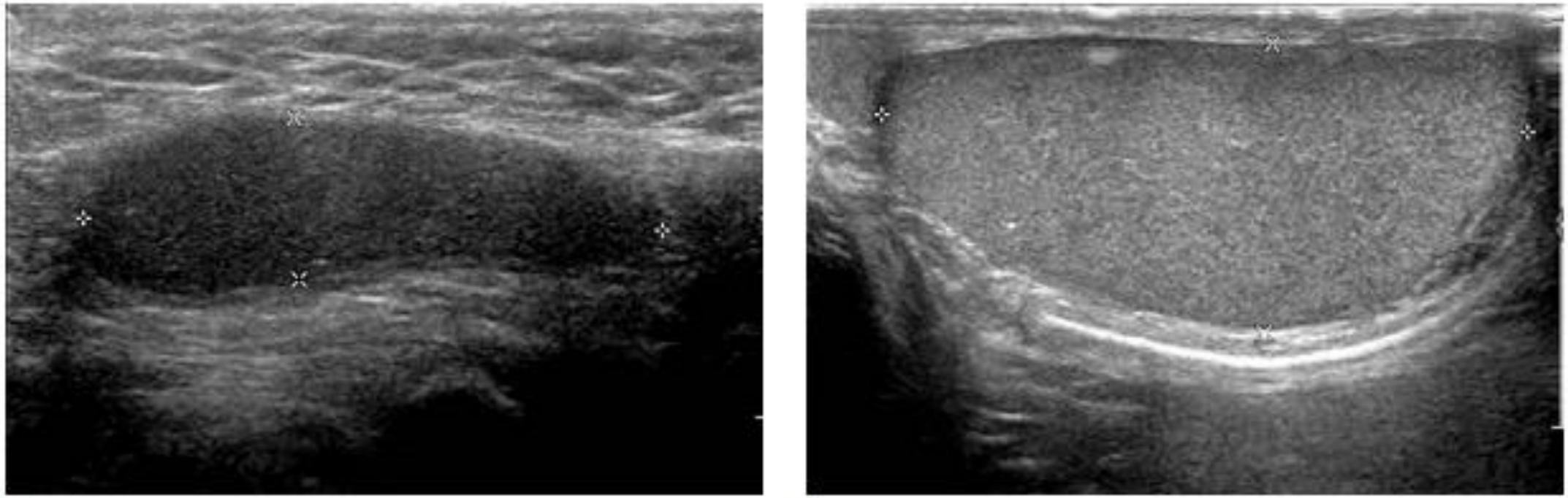

A B

Fig. 6. A 19-year-old man with right cryptorchidism.
A. Longitudinal ultrasonography shows a small, hypoechoic right testis in the right inguinal canal. B. Longitudinal ultrasonography shows a normal left testis.

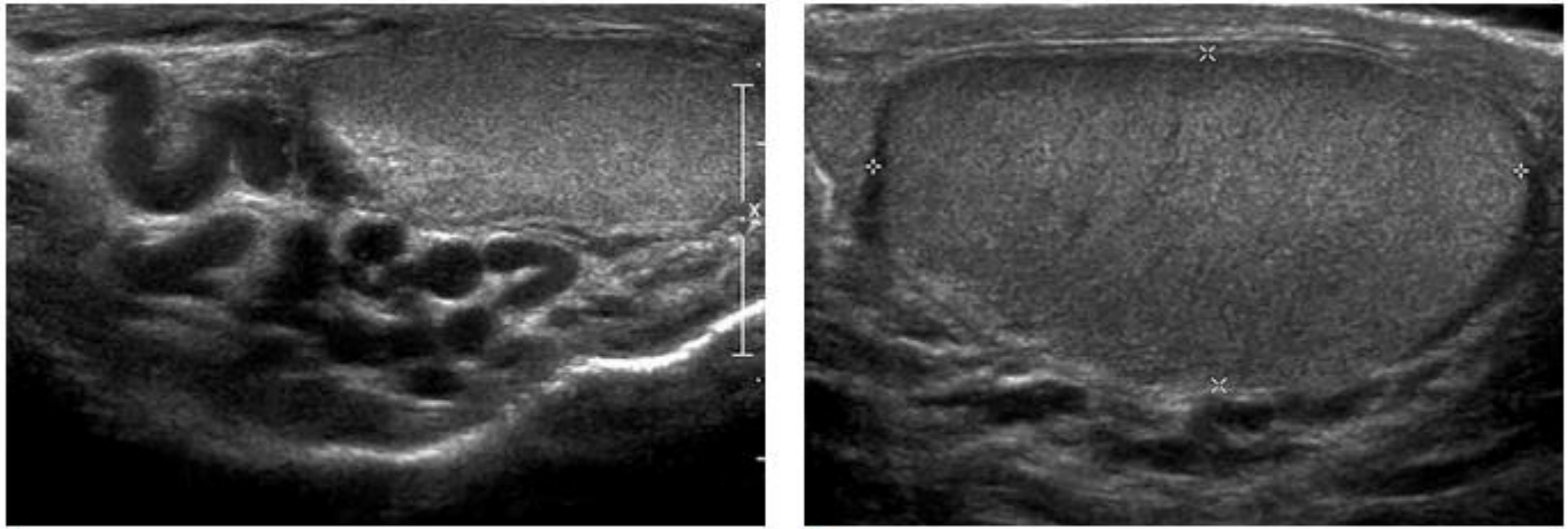

A B

Fig. 7. A 55-year-old man with varicocele.

A, B. Longitudinal ultrasonography shows that the left testis (A) is smaller (7.4 mL) than the right testis (11.2 mL) (B). There are multiple anechoic structures in the supratesticular region of the left testis.

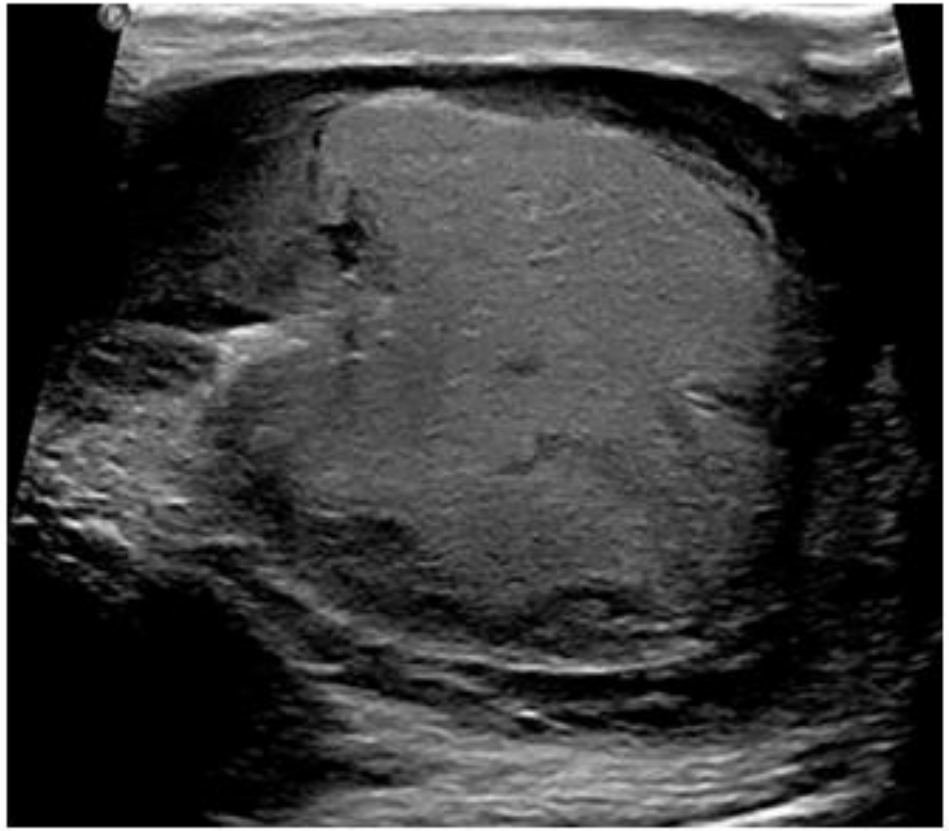

A

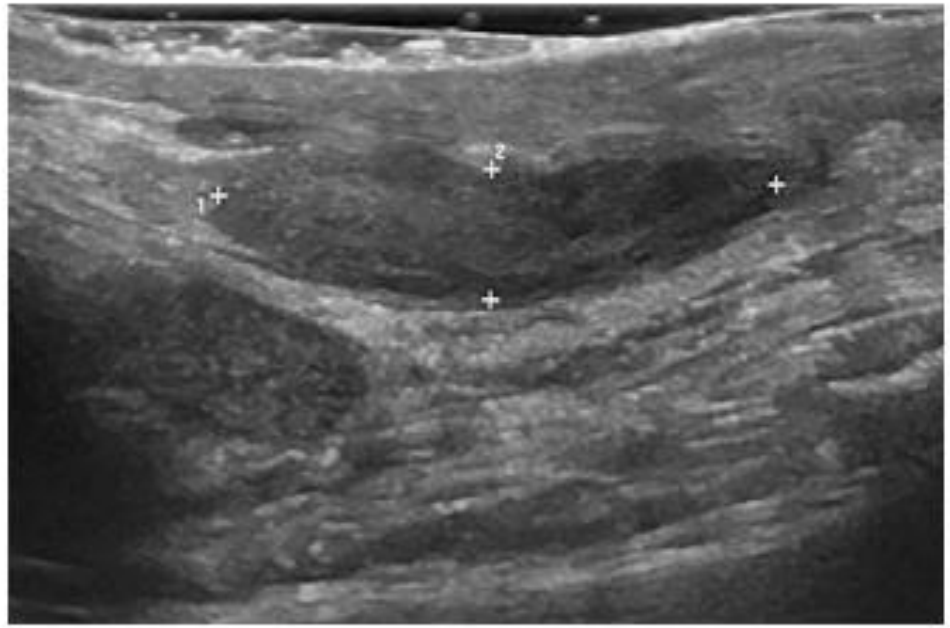

B

Fig. 8. A 28-year-old man with a right testicular contusion from trauma.

A. Longitudinal ultrasonography shows an enlarged, heterogeneously hypoechoic right testis with a 12-mL testicular volume. B. After 173 days, longitudinal ultrasonography shows a right testis reduced in volume (to 2.6 mL) with an oblong shape. The testis is heterogeneously hypoechoic on ultrasonography.

Conclusion

A wide range of conditions are associated with small testes, and radiologists should be aware of the variety of causes of this condition because ultrasonographic findings differ according to the underlying cause. Small testes in patients who experienced testicular torsion, mumps orchitis, or trauma usually showed heterogeneous echogenicity on ultrasonography. Relative to the normal testis, atrophic testes were homogeneously hypoechoic in patients with cryptorchidism and inguinal hernia and were isoechoic in patients with varicocele. Interestingly, most testes of Klinefelter syndrome patients had small hyperechoic or hypoechoic nodules, but the echogenicity of the remnant portion of the testes was homogeneous.

We suggest that heterogeneous echogenicity in small testes is due to testicular necrosis and hemorrhage caused by severe vascular compromise or trauma, such as testicular torsion, mumps orchitis, or other types of trauma. Homogeneous echogenicity in small testes is related to a lower degree of vascular compromise by extrinsic compression of the spermatic cord or testicular parenchyma in inguinal hernia cases and spermatogenesis failure resulting from elevated testicular temperatures in cases of cryptorchidism and varicocele.

Recurrence and additional treatment of cystic thyroid nodules after ethanol ablation: validation of three proposed criteria

Younghee Yim[1,2], Jung Hwan Baek[2], Sae Rom Chung[2], Young Jun Choi[2], Jeong Hyun Lee[2]

[1]Department of Radiology, Chung-Ang University Hospital, Chung-Ang University College of Medicine, Seoul; [2]Department of Radiology and Research Institute of Radiology, Asan Medical Center, University of Ulsan College of Medicine, Seoul, Korea

ULTRA SONO GRAPHY

ORIGINAL ARTICLE

https://doi.org/10.14366/usg.20039
pISSN: 2288-5919 • eISSN: 2288-5943
Ultrasonography 2021;40:378-386

Purpose: We evaluated the use of three criteria to determine the need for additional treatment of cystic thyroid nodules after their recurrence following ethanol ablation (EA).

Methods: In total, 154 patients (male:female=30:124; mean age, 53.4 years; range, 23 to 79 years) with 154 thyroid nodules (49 cystic and 105 predominantly cystic nodules) who presented between January 2014 and August 2017 were enrolled. All patients underwent follow-up ultrasonography (US) 1 month after EA, and were divided into therapeutic success and failure groups. Therapeutic success was defined as the absence of any residual fluid or sufficient volume reduction (≥50%) with improvement of nodule-related symptoms. The therapeutic failure was defined according to three previously suggested criteria for recommending additional treatment: nodules with ≥1 mL of remnant fluid (criterion 1), volume reduction <50% (criterion 2), and demonstration of a solid component with vascularity (criterion 3).

Results: Thyroid nodules treated by EA showed significant volume reduction (18.4±21.6 mL to 4.2±6.5 mL [1-month follow-up] to 1.9±3.3 mL [final follow-up], P<0.001) and improvement in clinical problems. Therapeutic failure were 26 patients according to criteria 1, 14 patients according to criteria 2, and 35 patients according to criteria 3. Additional treatment was unnecessary in 81.3%, 70.0%, and 77.8% of patients deemed to need it according to criteria 1, 2, and 3, respectively.

Conclusion: The choice to perform additional treatment after EA should be made according to a combination of clinical problems and US features. Understanding this concept will be useful in planning further treatment following US-guided EA.

Keywords: Thyroid nodules; Ethanol; Ablation; Recurrence

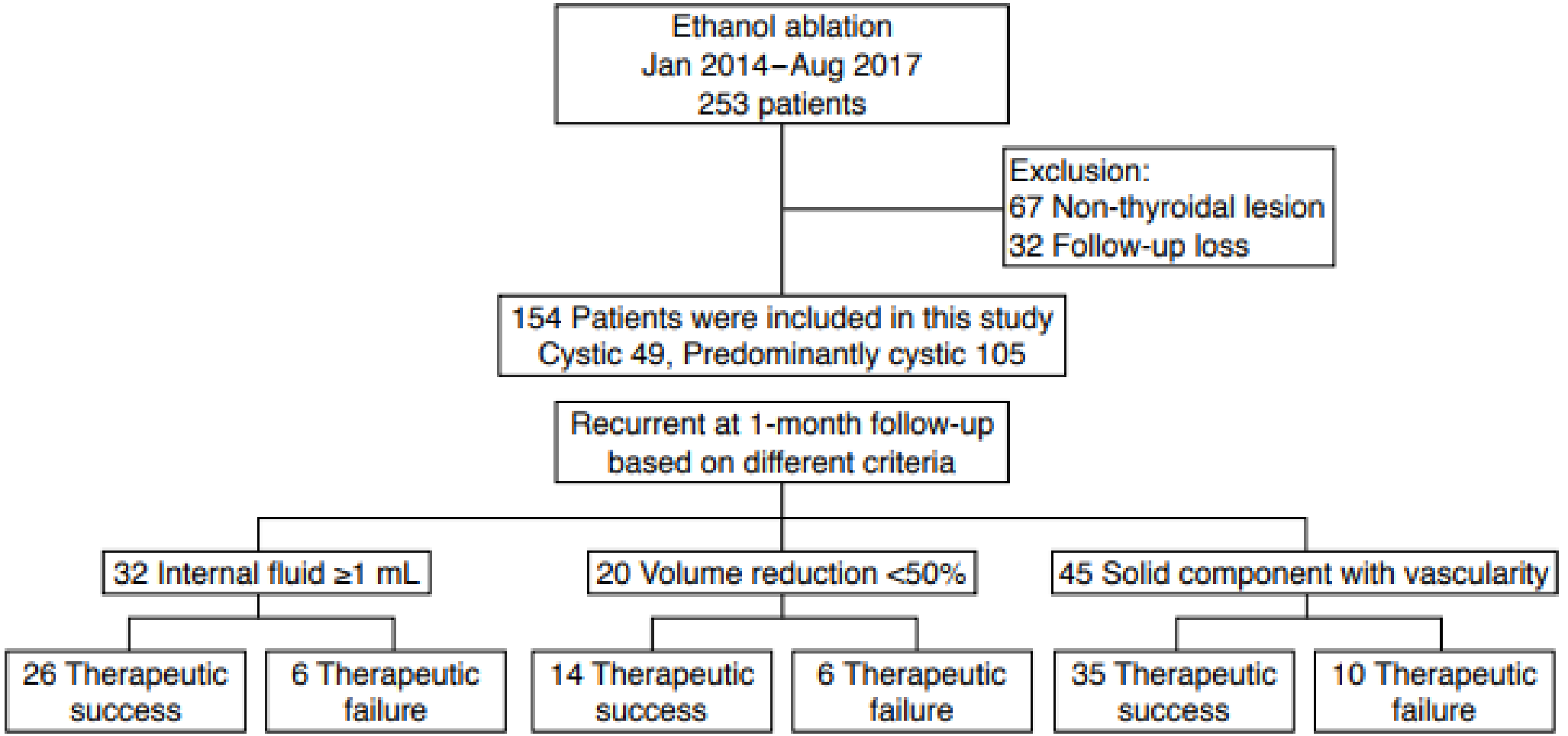

Fig. 1. Study population diagram.

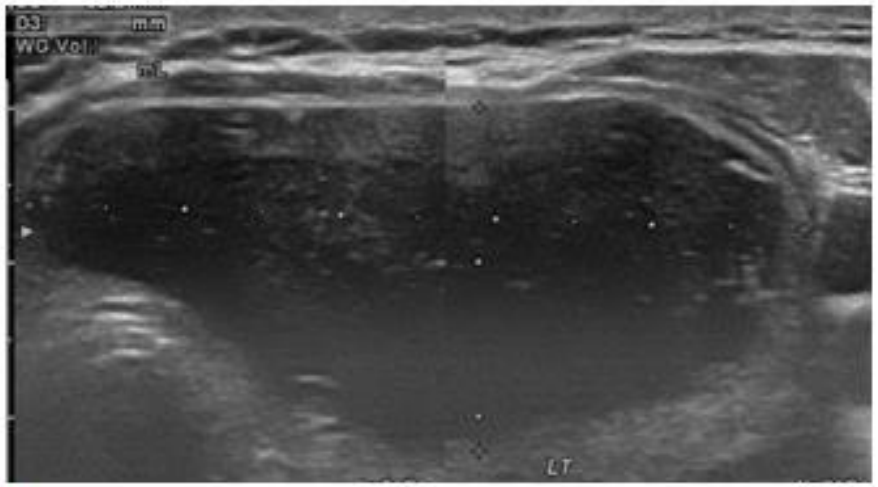

A

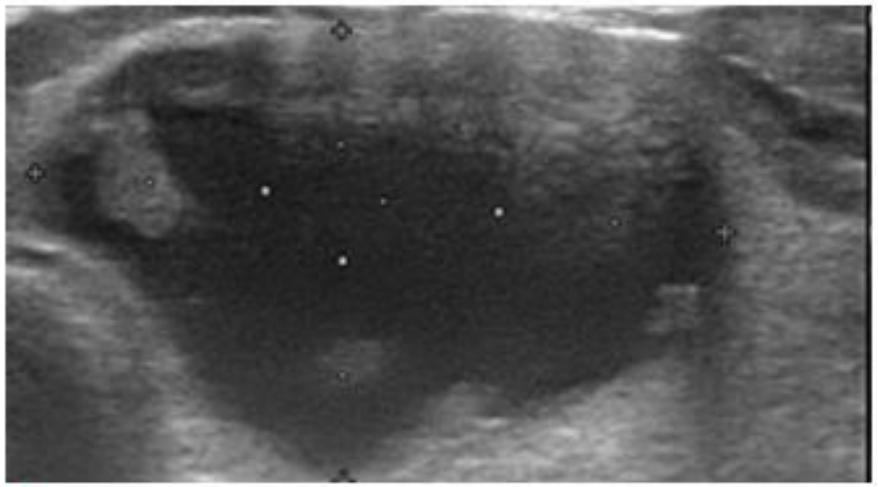

B

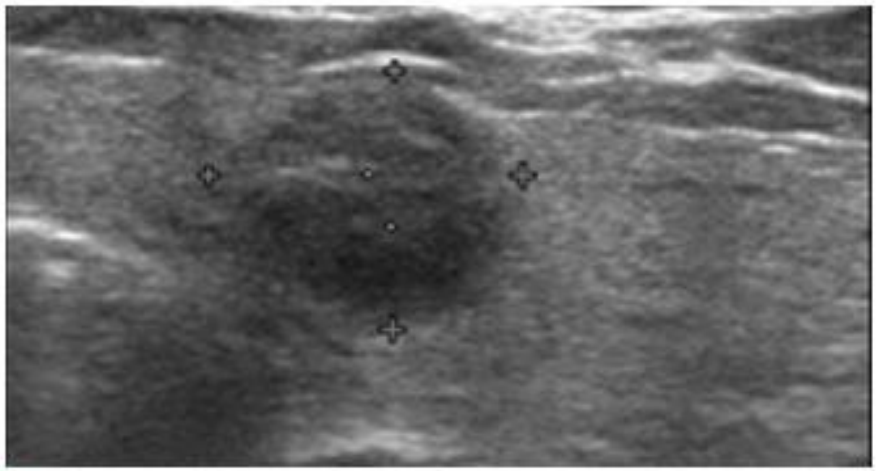

C

Fig. 2. A 64-year-old woman with thyroid cyst.
A. At the initial work-up, a predominantly cystic nodule was found, with benign cytology on fine-needle aspiration in the left thyroid gland with a volume of 28 mL. The initial cosmetic score and symptom score were both 4. The patient underwent ethanol ablation with 10 mL of ethanol followed by the aspiration of 25 mL of cystic contents. B. At a 1-month follow-up, the residual cystic volume was about 9 mL, but the symptoms had disappeared. C. The patient underwent regular follow-up rather than additional treatment, and the nodule had collapsed on 24-month follow-up ultrasonography (volume, 0.5 mL; volume reduction ratio, 98.2%).

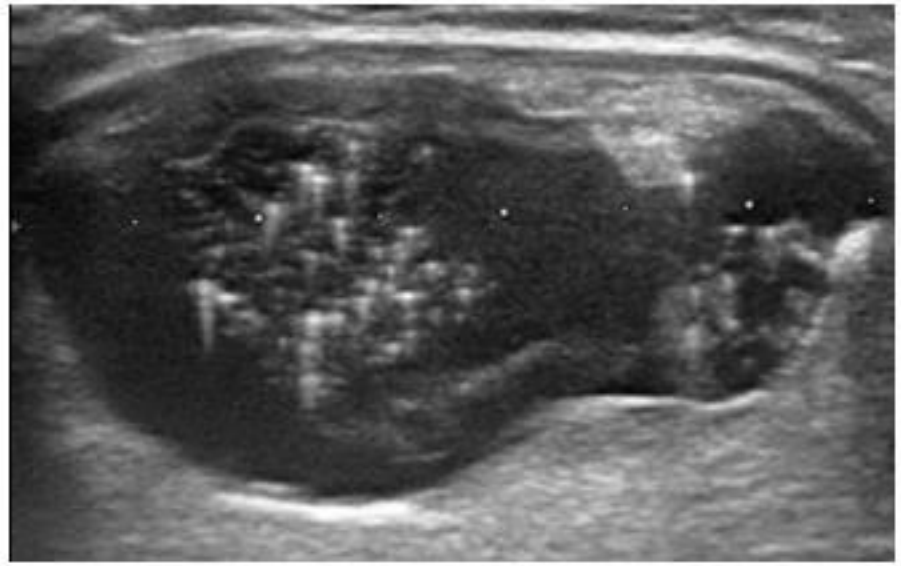

A

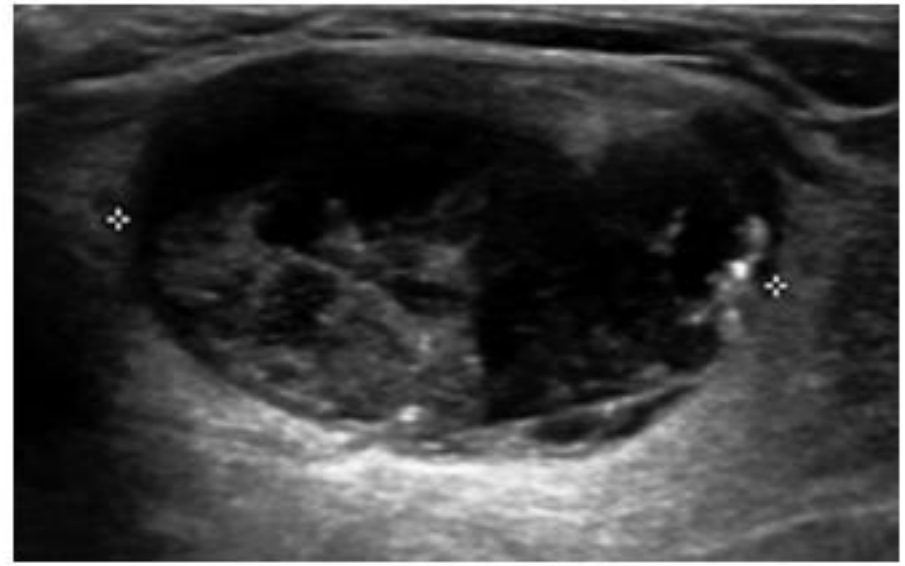

B

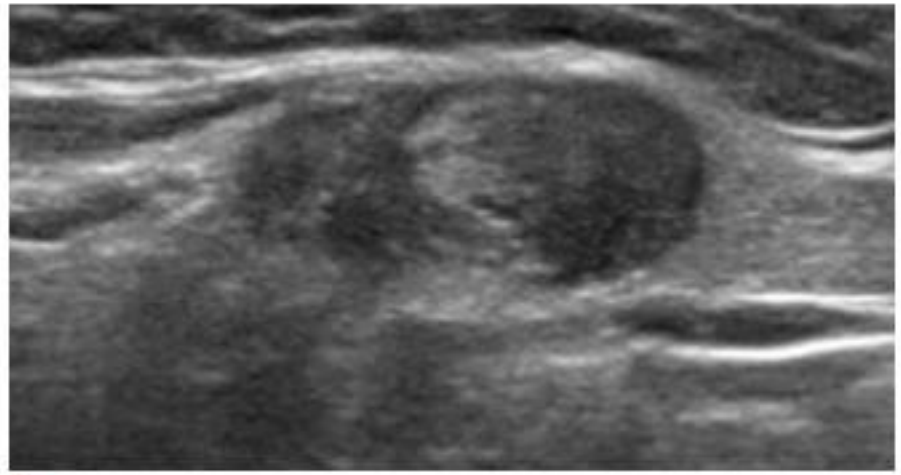

C

Fig. 3. A 71-year-old woman with predominantly cystic thyroid nodule. A. At the initial work-up, there was a predominantly cystic mass of about 10.8 mL with benign cytology on fine-needle aspiration in the left thyroid lobe. The initial cosmetic score was 4, and the symptom score was 2. The patient underwent ethanol ablation with 5 mL of ethanol followed by the aspiration of 10 mL of cystic contents. B. At a 1-month follow-up, the residual cystic volume was 7.4 mL, which was a <50% volume reduction. As she did not have any symptoms, the patient did not want to undergo additional treatment. C. She underwent regular follow-up without additional treatment, and the nodule had collapsed on 36-month follow-up ultrasonography (volume, 0.7 mL; volume reduction ratio, 93.5%).

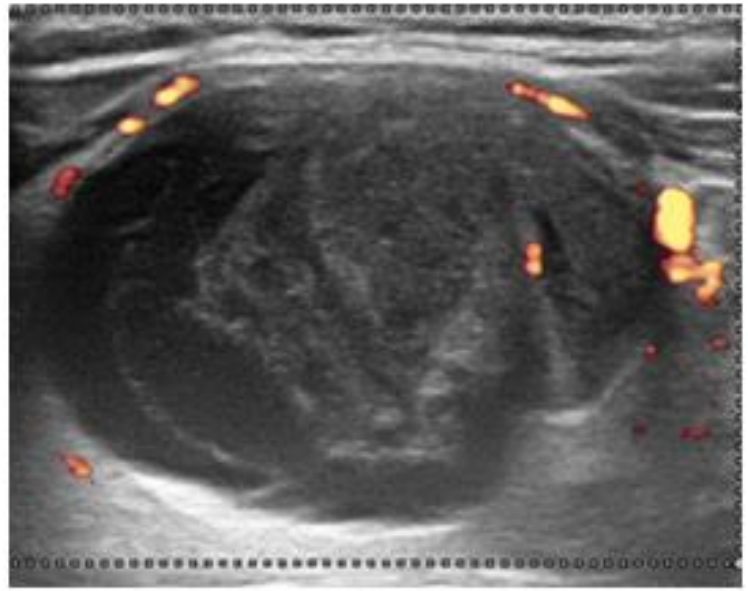

A

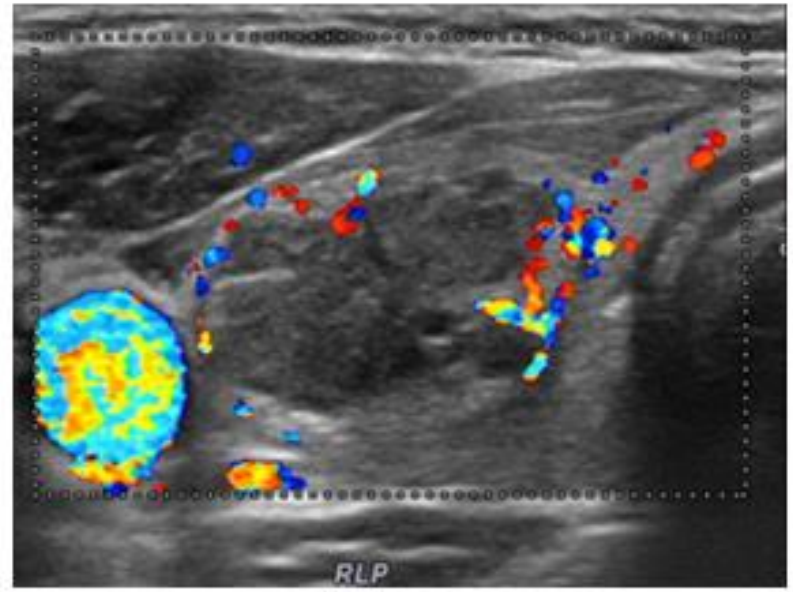

B

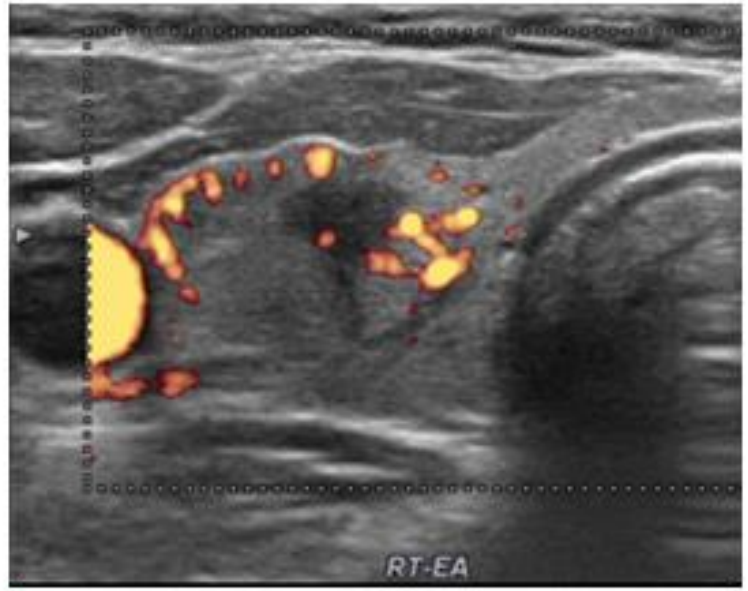

C

Fig. 4. A 63-year-old woman with predominantly cystic thyroid nodule.
A. At the initial work-up, there was a cystic mass of about 10 mL with benign cytology on fine-needle aspiration in the right thyroid lobe. The initial cosmetic score was 4, and the symptom score was 6. The patient underwent ethanol ablation with 5 mL of ethanol, followed by the aspiration of 10 mL of cystic contents. B. At a 1-month follow-up, the size of the nodule had significantly decreased (2.6 mL, 75.2% volume reduction ratio), but the nodule showed a solid component with vascularity (vascular grade 3) that was not definitely seen in the initial examination. As her symptoms had dramatically reduced to a symptom score of 2 after ethanol ablation, the patient underwent observation without additional treatment. C. At the 32-month follow-up, immediate additional treatment was still not necessary, as there were no symptoms (volume, 1.3 mL; volume reduction ratio, 87.6%), even though there might be the possibility of recurrence during long-term follow-up because of the solid component with vascularity.

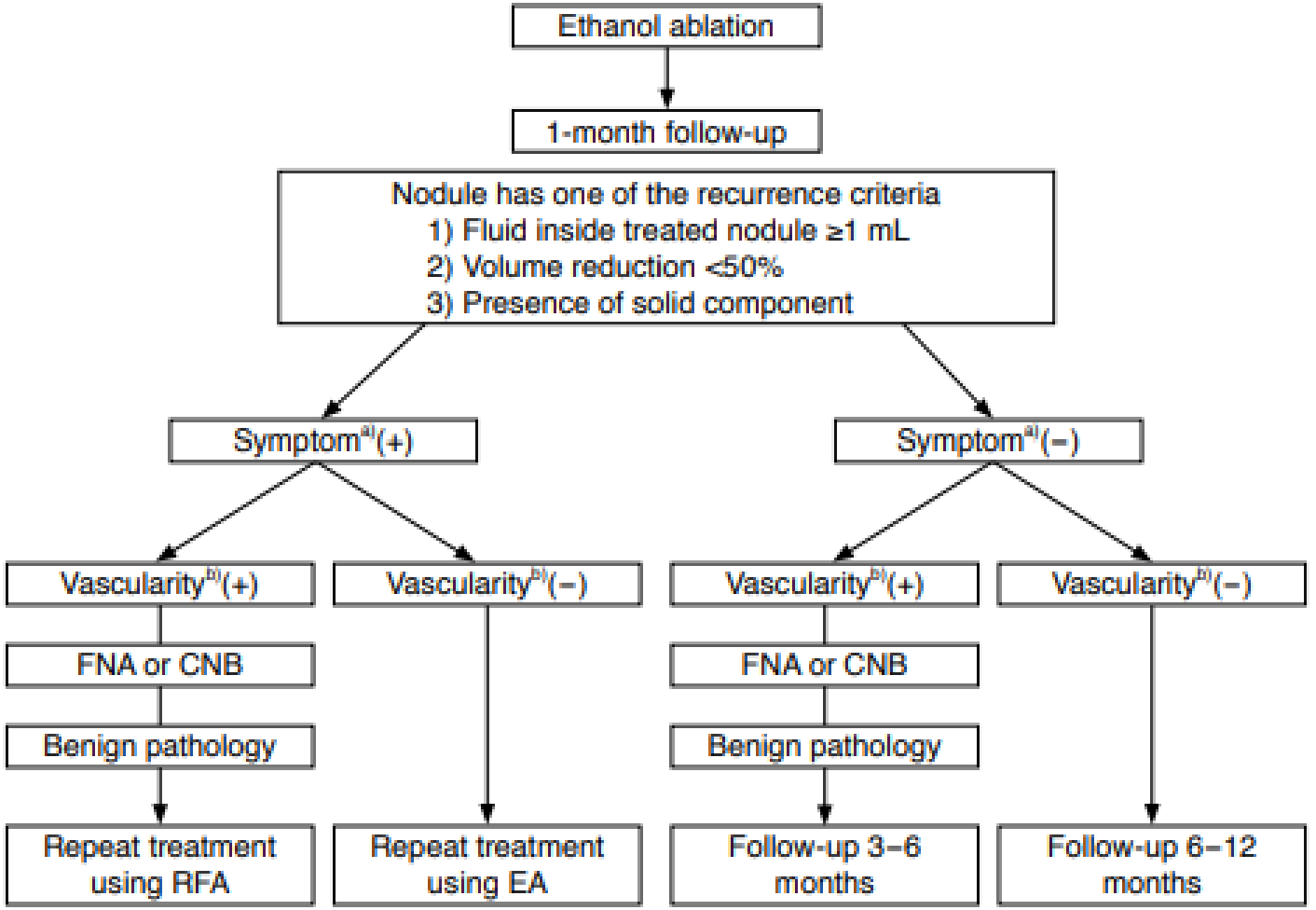

Fig. 5. Suggested additional treatment strategy after ethanol ablation (EA). FNA, fine-needle aspiration; CNB, core needle biopsy; RFA, radiofrequency ablation. [a]Symptom indicated on the figure includes cosmetic problems. [b]Vascularity includes intranodular vascularity (grades 3 and 4).

Evaluation of the ulnar nerve with shear-wave elastography: a potential sonographic method for the diagnosis of ulnar neuropathy

Sujin Kim, Guen Young Lee

Department of Radiology, Chung-Ang University Hospital, Seoul, Korea

ULTRA SONO GRAPHY

ORIGINAL ARTICLE

https://doi.org/10.14366/usg.20101
pISSN: 2288-5919 • eISSN: 2288-5943
Ultrasonography 2021;40:349-356

In conclusion, the ulnar nerve is stiffer in patients with cubital tunnel syndrome than in patients with lateral or medial epicondylitis. In addition, SWE seems to be a new reliable and simple quantitative diagnostic technique to aid in the precise diagnosis of ulnar neuropathy at the cubital tunnel.

Purpose: This study was designed to verify whether shear-wave elastography (SWE) can be used to differentiate ulnar neuropathy at the cubital tunnel from asymptomatic ulnar nerve or medial epicondylitis. An additional aim was to determine a cut-off value to identify patients with ulnar neuropathy.

Methods: This study included 10 patients with ulnar neuropathy at the cubital tunnel as confirmed with electromyography (three women and seven men; mean age, 51.9 years), 10 patients with medial epicondylitis (nine women and one man; mean age, 56.1 years), and 37 patients with asymptomatic ulnar nerve and lateral epicondylitis (21 women and 16 men; mean age, 54.0 years). Each patient underwent SWE of the ulnar nerve at the cubital tunnel, distal upper arm, and proximal forearm.

Results: Patients with ulnar neuropathy at the cubital tunnel exhibited significantly greater mean ulnar nerve stiffness at the cubital tunnel (66.8 kPa) than controls with medial epicondylitis (21.2 kPa, P=0.015) or lateral epicondylitis (33.9 kPa, P=0.040). No significant differences were observed between patients and controls with regard to ulnar nerve stiffness at the distal upper arm or the proximal forearm. A stiffness of 31.0 kPa provided 100% specificity, 80.0% sensitivity, 100% positive predictive value, and 83.3% negative predictive value for the differentiation between ulnar neuropathy and medial epicondylitis.

Conclusion: Cubital tunnel syndrome is associated with a stiffer ulnar nerve than lateral or medial epicondylitis. SWE seems to be a new, reliable, and simple quantitative diagnostic technique to aid in the precise diagnosis of ulnar neuropathy at the cubital tunnel.

Keywords: Ulnar neuropathy; Cubital tunnel syndrome; Medial epicondyle pain; Shear-wave elastography

A

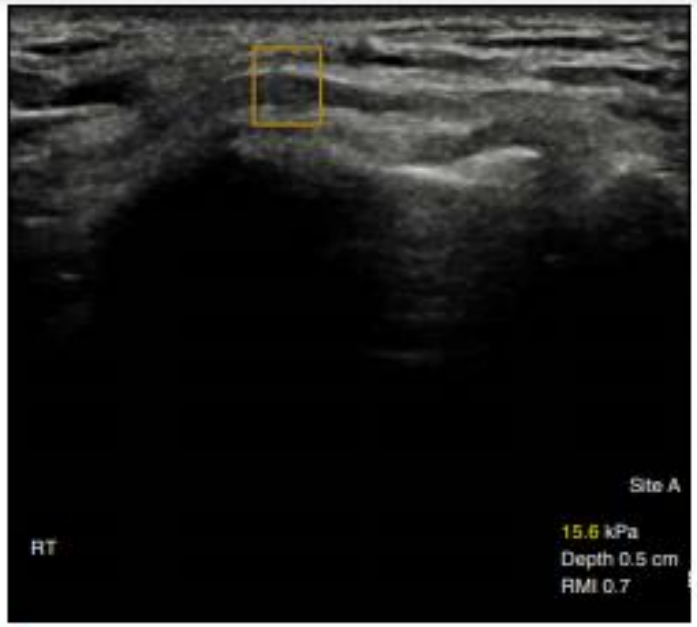

B

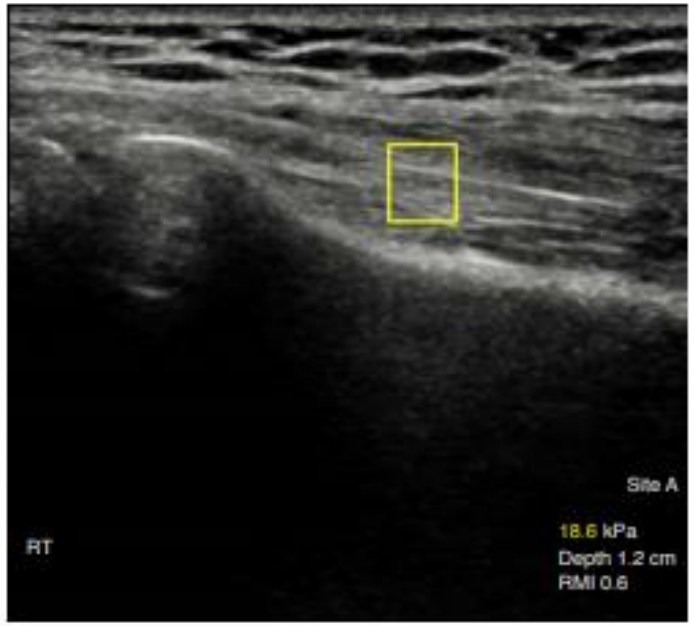

C

Fig. 1. A 58-year-old woman with right lateral epicondylitis.
Elastography images of the ulnar nerve at the elbow are shown. A. The shear-wave elastography (SWE) value of the ulnar nerve at the level of the distal upper arm was 7.2 kPa. B. The SWE value of the ulnar nerve at the level of the cubital tunnel was 15.6 kPa. C. The SWE value of the ulnar nerve at the level of the proximal forearm was 18.6 kPa. RMI, reliability measurement index.

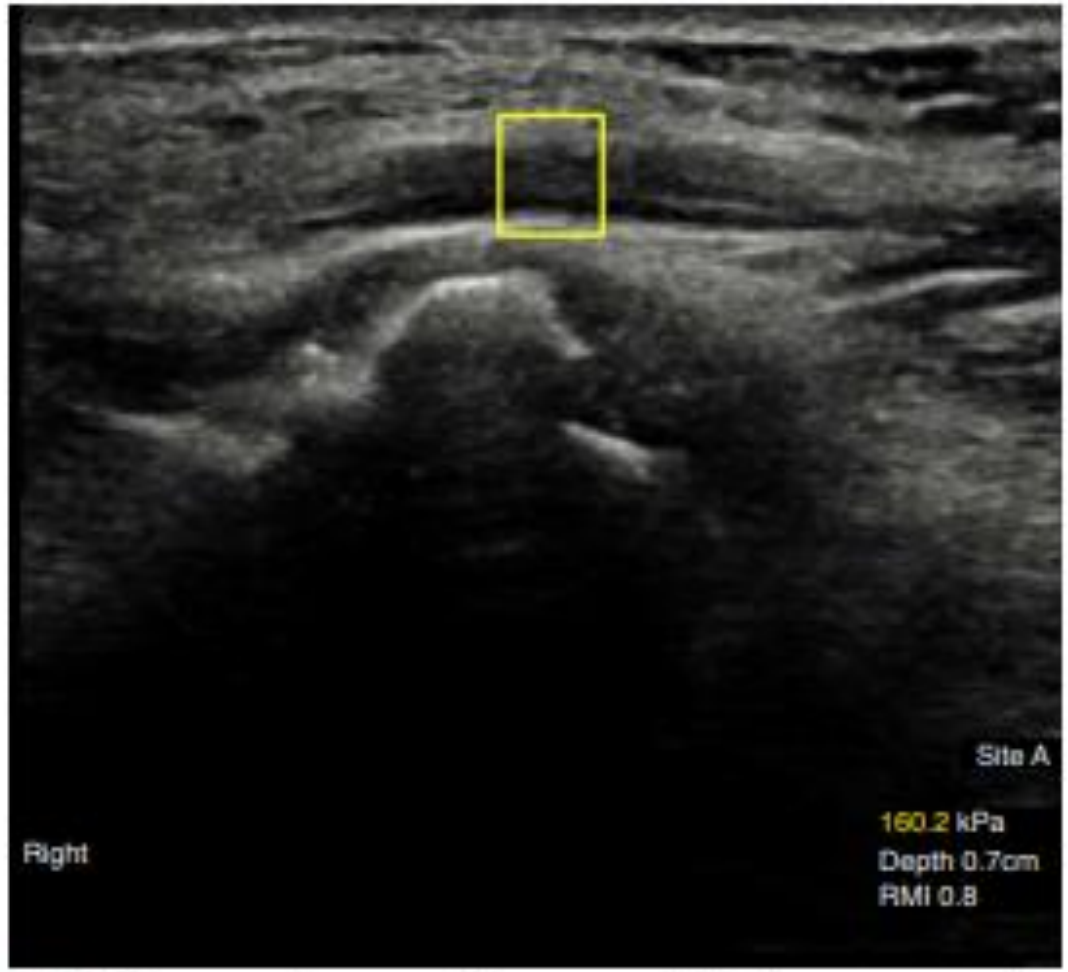

Fig. 2. **A 68-year-old man with severe right ulnar neuropathy on electromyography.** Elastographic presentation of the ulnar nerve at the level of the cubital tunnel is shown. The shear-wave elastography value of the ulnar nerve at the cubital tunnel was high (160.2 kPa). RMI, reliability measurement index.

Table 2. Mean CSA values by location in ulnar neuropathy, medial epicondylitis, and lateral epicondylitis

CSA value	Ulnar neuropathy	Medial epicondylitis	Lateral epicondylitis	P-value of three groups	P-value of ulnar neuropathy vs. no ulnar neuropathy
Proximal CSA (mm^2)	8.88±2.40	5.93±2.13	5.85±2.06	0.007	<0.001[a]
Tunnel CSA (mm^2)	13.73±7.24	8.02±3.78	8.96±3.51	0.081	0.002[a]
Distal CSA (mm^2)	7.49±3.00	4.85±1.00	5.61±2.45	0.094	0.038[b]

Values are presented as mean±SD.

CSA, cross-sectional area; SD, standard deviation.

[a]Statistical analysis was performed using the t test. [b]Statistical analysis was performed using the Mann-Whitney test.

Table 3. Mean SWE values and RMI by location in ulnar neuropathy, medial epicondylitis, and lateral epicondylitis

SWE value	Ulnar neuropathy	Medial epicondylitis	Lateral epicondylitis	P-value of three groups	P-value of ulnar neuropathy vs. no ulnar neuropathy[a]
Proximal pressure (kPa)	25.4±16.6	23.2±16.9	28.4±22.3	0.819	0.850
RMI	0.76±0.16	0.69±0.14	0.70±0.19	0.156	0.287
Tunnel pressure (kPa)	66.8±52.1	21.2±5.2	33.9±23.6	0.048	0.020
RMI	0.68±0.19	0.75±0.12	0.67±0.14	0.849	0.616
Distal pressure (kPa)	27.5±7.2	28.5±27.3	31.6±18.1	0.382	0.916
RMI	0.72±0.18	0.80±0.12	0.78±0.13	0.620	0.206
Tunnel/proximal pressure	3.41±2.76	1.46±1.08	2.30±3.31	0.075	0.025
Tunnel/distal pressure	2.57±2.32	1.12±0.66	1.35±1.33	0.072	0.022

SWE, shear-wave elastography; RMI, reliability measurement index.

[a]Statistical analysis was performed using the Mann-Whitney test.

Liver stiffness quantification in biopsy-proven nonalcoholic fatty liver disease patients using shear wave elastography in comparison with transient elastography

Adele Taibbi[1], Salvatore Petta[2], Domenica Matranga[3], Giovanni Caruana[1], Roberto Cannella[1], Gabriele Busè[1], Vito Di Marco[2], Massimo Midiri[1], Tommaso Vincenzo Bartolotta[1,4]

[1]Section of Radiology - BiND, University Hospital "Paolo Giaccone," Palermo; [2]Section of Gastroenterology and Hepatology, Department of Health Promotion Sciences Maternal and Infant Care, Internal Medicine and Medical Specialties, PROMISE, University of Palermo, Palermo; [3]Department of Health Promotion Sciences, Maternal and Infant Care, Internal Medicine and Medical Specialties "G. D'Alessandro," University of Palermo, Palermo; [4]Department of Radiology, Fondazione Istituto Giuseppe Giglio, Cefalù (Palermo), Italy

ULTRA SONO GRAPHY

ORIGINAL ARTICLE

https://doi.org/10.14366/usg.20147
pISSN: 2288-5919 • eISSN: 2288-5943
Ultrasonography 2021;40:407-416

Received: September 18, 2020
Revised: December 17, 2020
Accepted: December 18, 2020

In conclusion, TE and p-SWE had similar fair-to-good diagnostic performance for the diagnosis of biopsy-proven significant and advanced fibrosis in patients with NAFLD.

Purpose: This study prospectively assessed the performance of liver stiffness measurements using point shear-wave elastography (p-SWE) in comparison with transient elastography (TE) in patients with biopsy-proven nonalcoholic fatty liver disease (NAFLD).

Methods: Fifty-six consecutive adult patients with a histological diagnosis of NAFLD prospectively underwent TE and p-SWE on the same day. The median of 10 measurements (SWE-10), the first five (SWE-5), and the first three (SWE-3) measurements were analyzed for p-SWE. Liver biopsy was considered as the reference standard for liver fibrosis grade. Receiver operating characteristic (ROC) curves and areas under the ROC curves (AUROCs) were calculated to assess the performance of TE and p-SWE for the diagnosis of significant (F2–F4) and advanced fibrosis (F3–F4).

Results: Forty-six patients (27 men, 19 women; mean age, 54.7±9.1 years) had valid p-SWE and TE measurements. Twenty-seven patients (58.7%) had significant fibrosis and 18 (39.1%) had advanced fibrosis. For significant fibrosis, both SWE-10 (AUROC, 0.787; P=0.002) and SWE-5 (AUROC, 0.809; P=0.001) provided higher diagnostic performance than TE (AUROC, 0.719; P=0.016) and SWE-3 (AUROC, 0.714; P=0.021), albeit without statistical significance (P=0.301). For advanced fibrosis, SWE-5 showed higher diagnostic performance (AUROC, 0.809; P<0.001) than TE (AUROC, 0.799; P<0.001), SWE-10 (AUROC, 0.797; P<0.001), and SWE-3 (AUROC, 0.736; P=0.003), although the differences were not statistically significant (P=0.496). The optimal SWE-10 and SWE-5 cutoff values were ≥8.4 and ≥7.8 for significant fibrosis, and ≥9.1 and ≥8.8 for advanced fibrosis, respectively.

Conclusion: TE and p-SWE showed similar performance for the diagnosis of significant and advanced fibrosis in NAFLD patients.

Keywords: Nonalcoholic fatty liver disease; Nonalcoholic steatohepatitis; Shear wave elastography; Transient elastography; Liver stiffness

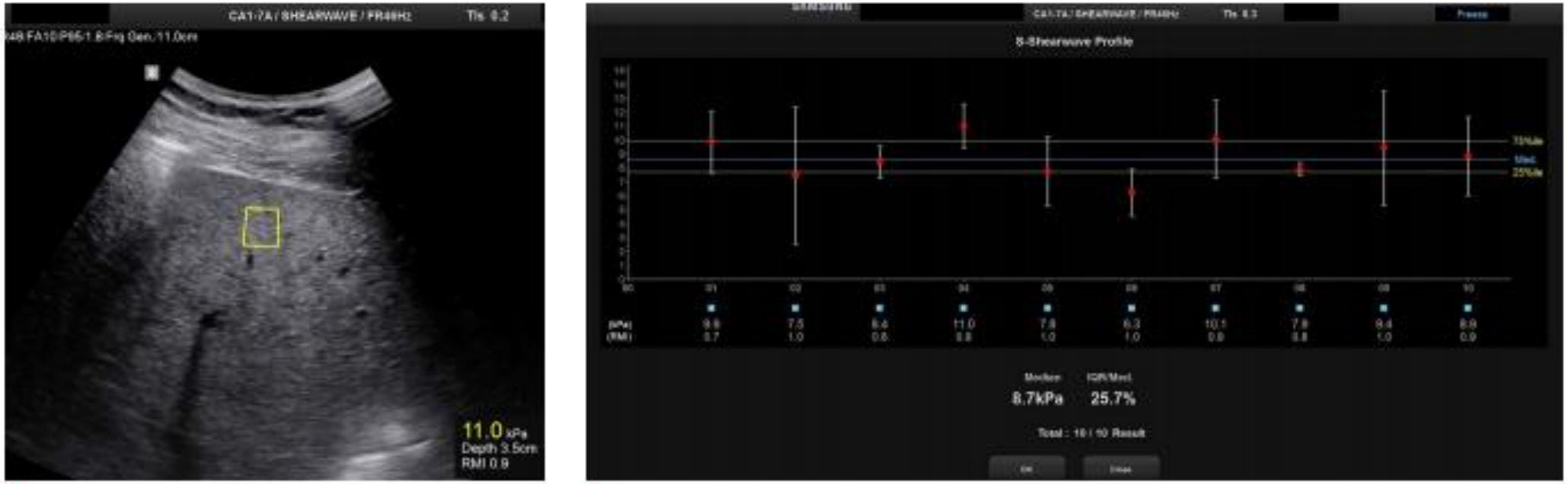

A B

Fig. 2. **Point shear-wave elastography in a 44-year-old man with significant fibrosis.**
A. Intercostal ultrasound image in the supine position shows a region of interest located under the liver capsule at a depth of 3.5 cm. B. Ten valid measurements are reported with a final median liver stiffness value of 8.7 kPa indicated in the lowest part of the image. A good interquartile range is also shown.

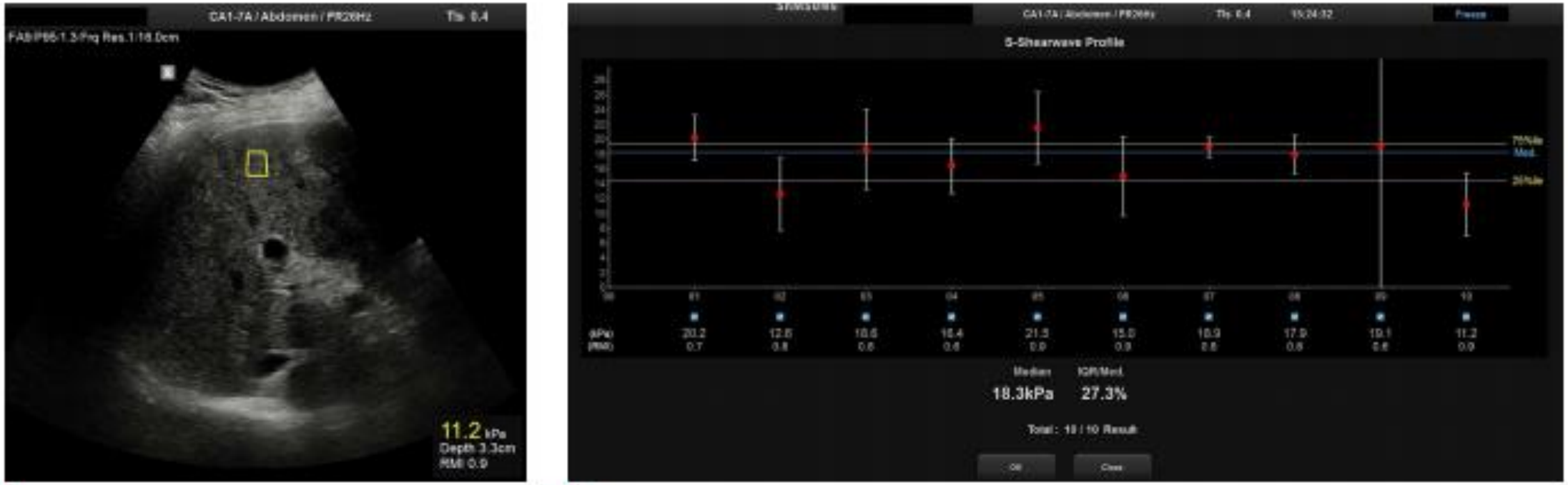

A B

Fig. 4. Point shear-wave elastography in a 69-year-old man with advanced fibrosis.
A. Intercostal ultrasound image in the supine position shows a region of interest located under the liver capsule at a depth of 3.3 cm. B. Ten valid measurements are reported with a final median liver stiffness value of 18.3 kPa, as indicated in the lowest part of the image. A good interquartile range is also shown.